OPTOELECTRONICS AND ADVANCED MATERIALS – RAPID COMMUNICATIONS Vol. 5, No. 6, June 2011, p. 596 - 599

$GdVO_4:Ln^{3+}$ (Ln = Eu, Dy, and Sm) microstructures: solvothermal and luminescent properties

FUHOU ZHENG, WENXIN WANG[a], PIAOPING YANG[a,*]
[a]*College of Science, Harbin Engineering University, Harbin 150001, P. R. China*
[b]*College of Material Science and Chemical Engineering, Harbin Engineering University, Harbin 150001, P. R. China*

$GdVO_4:Ln^{3+}$ (Ln= Eu, Dy, Sm) microstructures have been synthesized by a facile solvothermal route. X-ray diffraction (XRD), scanning electron microscopy (SEM), transmission electron microscopy (TEM), photoluminescence (PL) and kinetic decays were employed to characterize these samples. The results show that the as-synthesized phosphors are of high purity and crystallinity. SEM and TEM results indicate that the sample consists of quasi-spherical microparticles, which is composed of numerous tiny nano particles. Under ultraviolet (UV) excitation, $GdVO_4:Ln^{3+}$ phosphors show their strong characteristic emissions due to an efficient energy transfer from vanadate groups to the dopants.

(Received March 6, 2011; accepted June 9, 2011)

Keywords: $GdVO_4$, Luminescence, Ethylene glycol, Solvothermal

1. Introduction

Recently, rare earth doped vanadate inorganic salts have attracted much attention due to their widely utilization in lighting lamp, plasma display panel (PDP) phosphor, laser system and catalyst fields [1–5]. Because of the high luminescence quantum yields derived from f-f transitions, vanadate salts have been extensively studied as excellent host materials for doping various rare earth ions to emit a variety of colors [6–11]. Among all the rare earth ions doped vanadate salts, Eu^{3+} doped YVO_4 have gained much interest because of their commercial applications in color television, high-pressure mercury lamp, and a scintillator in medical detection as an important red-emitting phosphor. Besides, Dy^{3+} and Sm^{3+} ions can also act as useful activators. Dy^{3+}-doped YVO_4 is a potential white phosphor because of its yellow ($^4F_{9/2}\rightarrow{}^6H_{13/2}$) and blue ($^4F_{9/2}\rightarrow{}^6H_{15/2}$) emissions, and Sm^{3+}-doped YVO_4 emits characteristic red-orange emissions of Sm^{3+} at 567 ($^4G_{5/2}\rightarrow{}^6H_{5/2}$), 605 ($^4G_{5/2}\rightarrow{}^6H_{7/2}$), and 649 ($^4G_{5/2}\rightarrow{}^6H_{9/2}$) nm [12,13]. As a promising host material for rare earth ions activated phosphors with the similar structure to YVO_4, $GdVO_4$ based phosphors have also been investigated for their high photoluminescence (PL) and cathodoluminescence (CL) [2,14,15]. Up to data, several routes have been developed to fabricate rare earth ions doped vanadate salts phosphors, such as hydrothermal method, sol-gel technique, solution combustion synthesis, micro-emulsion route, electrospinning process, and microwave heating approach [16–20,11,13]. Among all the methods, hydrothermal method has proved a facile and economical process, which can synthesize phosphors with high crystallinity and narrow size distribution at a mild reaction condition without milling or further calcination treatment [16]. Furthermore, the morphology, structure, and the size of the as-synthesized phosphors can also be tuned by altering the reaction conditions, such as temperature, react time, pH value and other parameters.

In this paper, a facile solvothermal route has been presented to synthesize $GdVO_4:Ln^{3+}$ microstructures using ethylene glycol (EG) as solvent. $GdVO_4:Ln^{3+}$ phosphors have been successfully synthesized with well defined morphology and relatively narrow size distribution. Additionally, the luminescent properties and the decay times of different rare earth ions doped $GdVO_4$ phosphors have been investigated in detail by photoluminescence and the kinetic decays techniques. The photoluminescence properties indicate that zircon-type $GdVO_4:Ln^{3+}$ phosphors may be potential in luminescence applications.

2. Experimental section

2.1. Synthesis

All the reagents including Ethylene glycol (EG) (A. R., Beijing Beihua Chemical Co., Ltd.), sodium acetate ($C_2H_3NaO_2$) (A. R., Beijing Jingyi Chemical Co., Ltd.), ammonium metavanadate (NH_4VO_3) (A. R., Tianjin Damao Chemical Co., Ltd.), Y_2O_3, Eu_2O_3, Dy_2O_3, Sm_2O_3 (99.99%, Science and Technology Parent Company of Changchun Institute of Applied Chemistry), HNO_3 (A. R., Beijing Beihua Chemical Co., Ltd.) were analytical grade and used without further purification. $Ln(NO_3)_3$ (Ln= Eu, Dy, and Sm) were obtained from their corresponding oxides by dissolving stoichiometric Ln_2O_3 in dilute HNO_3 solution under heating with agitation. The superfluous HNO_3 was driven off until the $Ln(NO_3)_3$ crystal powders were obtained.

In a typical process for the synthesis of $GdVO_4:Eu^{3+}$ crystals with the Eu^{3+} doping concentration of 5 mol%, 1 mmol of $(NH_4)_3VO_3$ was dissolved in a mixed solution containing 1 mL of HNO_3, 2 mL of H_2O, then 2 g of sodium acetate and 0.95 mmol $Gd(NO_3)_3$ and 0.05 mmol as-prepared $Eu(NO_3)_3$ were added into the solution. Subsequently, 34 mL of EG was added into the solution. After stirring for 2 h, the obtained solution was transferred into a 50 mL Teflon-lined autoclave, and heated at 180 °C for 12 h. After the autoclave was naturally cooled to the room temperature, the final products were separated by centrifugation, and the precipitates were washed several times with ethanol at 4500 rpm for 15 min. Finally, the obtained samples were dried in vacuum at 60 °C for 24 h. Sm^{3+} and Dy^{3+} doped $GdVO_4$ phosphors were synthesized by the same process except for 5 mol% Eu^{3+} has been replaced by 3 mol% Dy^{3+} and 1 mol% Sm^{3+}.

2.2. Characterization

Powder X-ray diffraction (XRD) patterns were obtained on a Rigaku TTR III diffractometer using Cu Kα radiation (λ = 0.15405 nm), operating at 40 kV and 150 mA. Fourier-transform IR spectra were recorded on a Perkin-Elmer 580B IR spectrophotometer using KBr pellet technique. Transmission electron microscope (TEM) and high-resolution transmission electron microscope (HRTEM) images were recorded on a FEI Tecnai G^2 S-Twin with an acceleration voltage of 200 kV. The X-ray photoelectron spectra (XPS) were taken on a VG ESCALAB MK II electron energy spectrometer using Mg Kα (1253.6 eV) as the X-ray excitation source. Photoluminescence (PL) excitation and emission spectra were recorded with a Hitachi F-4500 spectrophotometer equipped with a 150 W xenon lamp as the excitation source. Luminescence decay curves were obtained from a Lecroy Wave Runner 6100 digital oscilloscope (1 GHz) using a 250 nm laser (pulse width = 4 ns, gate = 50 ns) as the excitation source (Continuum Sunlite OPO). All the measurements were performed at room temperature.

3. Result and discussion

3.1. Crystallinity, structure and phase purity

Fig. 1 shows the XRD patterns of the as-synthesized $GdVO_4:Eu^{3+}$, $GdVO_4:Sm^{3+}$, and $GdVoO_4:Dy^{3+}$ phosphors, respectively. Vertical bars show the standard tetragonal bulk $GdVO_4$ (JCPDS 86–0996) for comparison. As shown, all the XRD patterns for the three samples can be directly indexed to a pure tetragonal structure (I41/a space group). In addition, no other impurities related with the doped components can be observed s, suggesting that the rare earth ions have been uniformly incorporated into the host lattice of $GdVO_4$. The calculated cell constants of a = 7.1586 Å, c = 6.3417 Å for $GdVO_4:Eu^{3+}$, a = 7.1658 Å, c = 6.3387 Å for $GdVO_4:Dy^{3+}$, and a = 7.1850 Å, c = 6.3424 Å for $GdVO_4:Sm^{3+}$ are well consistent with the standard data of a = 7.2122 Å, c = 6.346 Å for pure tetragonal $GdVO_4$ (JCPDS 86–0996). The slight difference of the cell constants can be due to the ion sizes of the doped rare earth ions. It should be noted that the XRD diffractions peaks show some broadening, exhibiting the small size nature of the samples. The peak broadening can be used to estimate the average crystallite sizes by the Scherrer formula, $D = 0.89\lambda/\beta\cos\theta$, where D is the average grain size, λ is the X-ray wavelength (0.15405 nm), and θ and β are the diffraction angle and full-width at half-maximum (FWHM), respectively. The average crystallite sizes for $GdVO_4:Eu^{3+}$, $GdVO_4:Sm^{3+}$ and $GdVO_4:Dy^{3+}$ were calculated be about 18.7 nm, 17 nm and 22.2 nm, respectively. From Fig. 2d, the EDS analysis confirms the presence of V, Gd and O. The atomic percentage of V, Gd and O is 16.2, 17.3, and 66.3, respectively. Thus, the calculated atomic ratio of V/Gd/O is 1/1.08/4.09, which is consistent with the theoretical atomic V/Gd/O ratio (1/1/4).

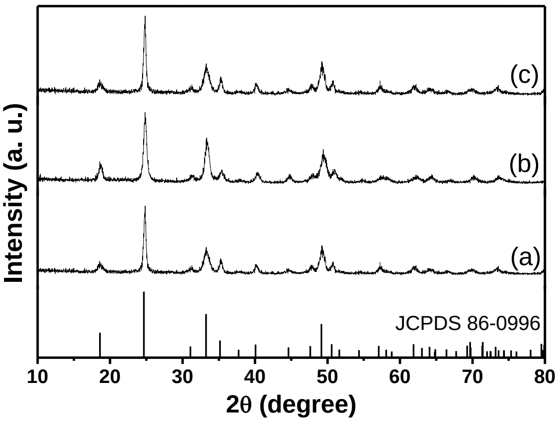

Fig. 1. XRD patterns of the as-synthesized $GdVO_4:Eu^{3+}$ (a), $GdVO_4:Dy^{3+}$ (b), $GdVO_4:Sm^{3+}$ (c), and the standard data for tetragonal $GdVO_4$ (JCPDS 86-0996).

3.2. Morphology, size and composition

The morphology, size and microstructure details were investigated by SEM and TEM techniques. The representative SEM images with different magnification, TEM image, HRTEM image, and EDS of $GdVO_4:Eu^{3+}$ are given in Fig. 2. From SEM images (Fig. 2a,b), we can see that the as-synthesized sample consists of relatively uniform spherical microstructure with the particle size of about 800 nm. TEM image (Fig. 2c) reveals that the microstructure is composed of many tiny nano-particles with loose structure, which is in agreement with the XRD result. Besides, the obvious lattice fringes in the HRTEM image (Fig. 2d) show the crystalline nature of the sample.

The calculated interplanar distance of 0.33 nm (marked by the arrows) between the adjacent lattice fringes corresponds to the (112) plane spacing of pure $GdVO_4$ (JCPDS 86–0996).

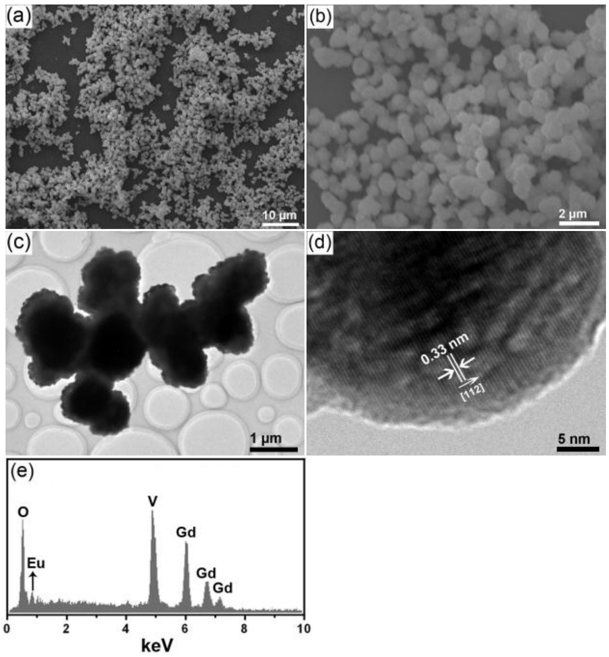

Fig. 2. SEM images (a, b), TEM image (c), HRTEM image (d) and EDS of the as-synthesized $GdVO_4:Eu^{3+}$.

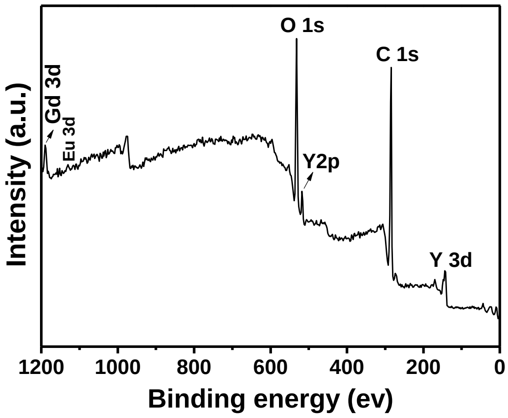

Fig. 3. XPS of as-synthesized $GdVO_4:Eu^{3+}$.

XPS technique has been tested as an effective tool for qualitatively determining the surface composition of a material. In the XPS spectrum (Fig. 3) of $GdVO_4:Eu^{3+}$, the binding energy of Eu 3d (1130 eV), Gd 3d (1221 eV), V 2p (518 eV), O 1s (531 eV), C 1s (284 eV) and Y 3d (169 eV) can be obviously found. By combination of previous XRD results, it can be deduced that these signals can be assigned to $GdVO_4:Eu^{3+}$. XPS results provide the additional evidence for the successful doping of Eu^{3+} in $GdVO_4$ lattice.

3.3. Photoluminescence (PL) properties

Fig. 4 shows the PL spectra of $GdVO_4:Eu^{3+}$, $GdVO_4:Dy^{3+}$, $GdVO_4:Sm^{3+}$, respectively. In the excitation spectrum of $GdVO_4:Eu^{3+}$ (Fig. 4a, left), the broad peak at 277 nm can be ascribed to the charge transfer band from the oxygen ligands to the central vanadium atom in the $GdVO_4$ host. Upon 277 nm ultraviolet (UV) excitation, the emission spectrum consists of a sharp peak (618 nm) and several weak lines (537 nm, 593 nm, 649 nm, and 698 nm), which can be assigned to the intrinsic transitions of $^5D_0 \rightarrow {}^7F_2$, $^5D_1 \rightarrow {}^7F_1$, $^5D_0 \rightarrow {}^7F_1$, $^5D_0 \rightarrow {}^7F_3$ and $^5D_0 \rightarrow {}^7F_4$, respectively [11,13,18]. According to magnetic dipole selection rules, the $^5D_0 \rightarrow {}^7F_2$ is electric-dipole-allowed owing to an admixture of opposite parity $4f^{n-1}d$ states by an odd parity crystal-field component. Therefore, its intensity is sensitive to the local structure around Eu^{3+} ions [21]. Obviously, the emission spectrum is dominated by the hypersensitive $^5D_0 \rightarrow {}^7F_2$ transition, which is the origin of the sample exhibits red luminescence.

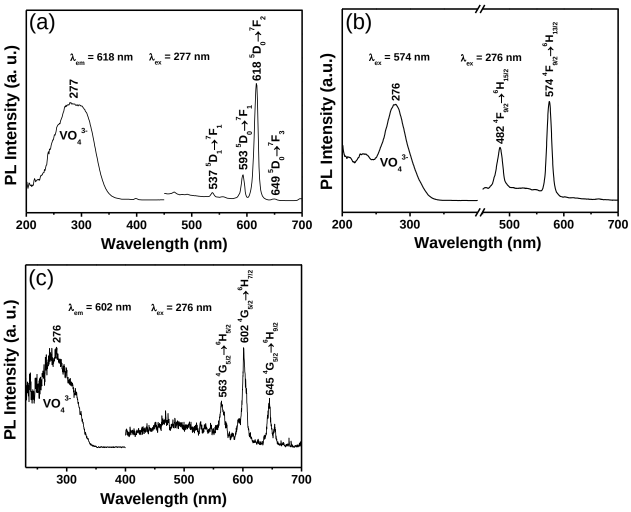

Fig. 4. The excitation (left) and emission spectra (right) of $GdVO_4:Eu^{3+}$ (a), $GdVO_4:Dy^{3+}$ (b), and $GdVO_4:Sm^{3+}$ (c).

The PL spectra of $GdVO_4:Dy^{3+}$ and $GdVO_4:Sm^{3+}$ are given in Fig. 4b and Fig. 4c, respectively. In the excitation spectrum (Fig. 4b, left) for $GdVO_4:Dy^{3+}$, the broad band with a maximum at 276 nm can be due to VO_4^{3-} absorption. From the emission spectrum upon 276 nm excitation (Fig. 4b, right), two characteristic peaks from $^4F_{9/2} \rightarrow {}^6H_{15/2}$ (482 nm, blue) and $^4F_{9/2} \rightarrow {}^6H_{13/2}$ (574 nm, yellow) are obvious, which can also be due to an efficient energy transfer from the VO_4^{3-} group to Dy^{3+} in $GdVO_4:Dy^{3+}$ [12,13]. The stronger intensity of the yellow emission than the blue emission can be attributed to the D_{2d} point symmetry of Dy^{3+} ions without an inverse center in the host of $GdVO_4$. A strong band with a maximum at 276 nm associated with the absorption of the VO_4^{3-} group can be detected in the excitation spectrum of $GdVO_4:Sm^{3+}$ (Fig. 4c, left). Excitation into the vanadate group at 276 nm yields the characteristic orange emission of Sm^{3+} at 563 nm ($^4G_{5/2}\rightarrow{}^6H_{5/2}$), 602 nm ($^4G_{5/2}\rightarrow{}^6H_{7/2}$), and 645 nm ($^4G_{5/2}\rightarrow{}^6H_{9/2}$) (Fig. 5c, right). No emission from the VO_4^{3-} groups can be observed, indicating an efficient energy transfer from VO_4^{3-} to Sm^{3+} [12,13]. The $^4G_{5/2}\rightarrow{}^6H_{5/2}$ (602 nm) transition is the predominant emission for $GdVO_4$:Sm^{3+}.

The corresponding CIE (Commission Intemationale de I'Eclairage 1931 chromaticity) coordinates positions of $GdVO_4$:Eu^{3+}, $GdVO_4$:Dy^{3+} and $GdVO_4$:Sm^{3+} are presented in Fig. 5, which show different emission colors. The $GdVO_4$:Eu^{3+} sample emits red light and its chromaticity coordinates are x = 0.5861, and y = 0.2966 (point a). The CIE coordinates for the emission spectrum of $GdVO_4$:Dy^{3+} are determined to be x = 0.3102 and y = 0.3933, locates in the blue-yellow region (point b). The $GdVO_4$:Sm^{3+} sample shows the orange luminescence color, and the chromaticity coordinates are x = 0.4661, and y = 0.3029 (point c). Furthermore, the typical decay curves for the luminescence of Eu^{3+} in $GdVO_4$:Eu^{3+}, Dy^{3+} in $GdVO_4$:Dy^{3+}, and Sm^{3+} in $GdVO_4$:Sm^{3+} have also been measured. The average lifetime for $^5D_0\rightarrow{}^7F_2$ (612 nm) of Eu^{3+}, $^4F_{9/2}\rightarrow{}^6H_{13/2}$ (572 nm) of Dy^{3+}, and $^4G_{5/2}\rightarrow{}^6H_{5/2}$ (602 nm) of Sm^{3+} in the $GdVO_4$ host lattices are determined to be 0.58, 0.11, and 0.37 ms, respectively.

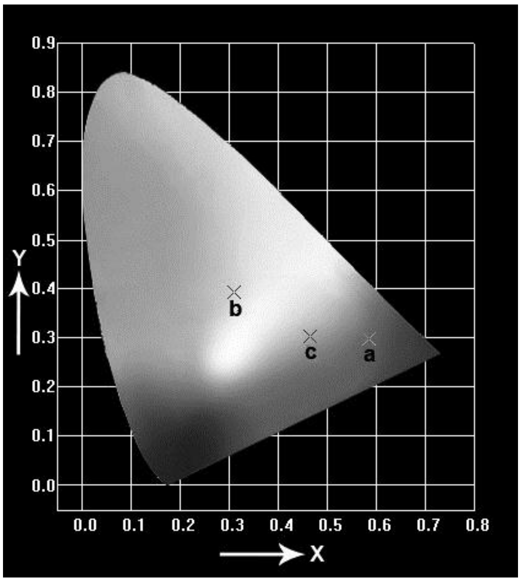

Fig. 5. CIE chromaticity diagram showing the emission colors for $GdVO_4$:Eu^{3+} (a), $GdVO_4$:Dy^{3+} (b), and $GdVO_4$:Sm^{3+} (c).

4. Conclusions

In summary, Eu^{3+}, Dy^{3+}, and Sm^{3+} doped $GdVO_4$ microstructures have been successfully synthesized by a facile solvothermal process using EG as solvent. The as-synthesized phosphors exhibit high purity and uniform morphology. The characteristic emission lines of Eu^{3+}, Dy^{3+} and Sm^{3+} are observed for the $GdVO_4$:Ln^{3+} (Ln = Eu, Dy, and Sm) phosphors, respectively. The phosphors show a potential application in the display fields based on their size, morphology and luminescent properties.

Acknowledgments

This project is financially supported the National Natural Science Foundation of China (NSFC 20871035), China Postdoctoral Special Science Foundation (200808281), and Harbin Sci.-Tech. Innovation Foundation (No. 2009RFQXG045).

References

[1] G. Wang, W. Qin, D. Zhang, L. Wang, G. Wei, P. Zhu, R. Kim, J. Phys. Chem. C **112**, 17042 (2008).
[2] C. C. Wu, K. B. Chen, C. S. Lee, T. M. Chen, B. M. Cheng, Chem. Mater. **19**, 3278 (2007).
[3] J. D. Pless, N. Erdman, D. Ko, L. D. Marks, P. C. Stair, K. R. Poeppelmeier, Cryst. Growth Des. **3**, 615 (2003).
[4] H. Wang, M. Yu, C. Lin, J. Lin, J. Colloid Inter. Sci. **300**, 176 (2006).
[5] C. R. Ronda, J. Alloys Compd. **225**, 534 (1995).
[6] A. Huignard, T. Gacoin, J. P. Boilot, Chem. Mater. **12**, 1090 (2000).
[7] K. Riwotzki, M. Haase, J. Phys. Chem. B **102**, 10129 (1998).
[8] K. Oka, H. Unoki, H. Shibata, H. Eisaki, J. Cryst. Growth **286**, 288 (2006).
[9] H. Zhang, X. Fu, S. Niu, Q. Xin, J. Alloys Compd. **457**, 61 (2008).
[10] Y. Kuisheng, Z. Fang, W. Rina, L. Hansheng, Z. Xiyan, J. Rare Earth. **24**,162 (2006).
[11] M. Yu, J. Lin, J. Fang, Chem. Mater. **17**, 1783 (2005).
[12] G. Wang, W. Qin, D. Zhang, L. Wang, G. Wei, P. Zhu, R. Kim, J. Phys. Chem. C **112**, 17042 (2008).
[13] Z. Hou, P. Yang, C. Li, L. Wang, H. Lian, Z. Quan, J. Lin, Chem. Mater. **20**, 6686 (2008).
[14] M. Gu, Q. Liu, S. Mao, D. Mao, C. Chang, Cryst. Growth Des. **8**, 1422 (2008).
[15] Q. L. Zhang, C. X. Guo, C. S. Shi, S. Z. Lu, J. Alloys Compd. **309**, 10 (2000).
[16] Z. Xu, X. Kang, C. Li, Z. Hou, C. Zhang, D. Yang, G. Li, J. Lin, Inorg. Chem. **49**, 6706 (2010).
[17] L. Sun, Y. Zhang, J. Zhang, C. Yan, C. Liao, Y. Lu, Solid Stat. Commun. **124**, 35 (2002).
[18] M. Yu, J. Lin, Z. Wang, J. Fu, S. Wang, H. J. Zhang, Y. C. Han, Chem. Mater. **14**, 2224 (2002).
[19] S. Ekambaram, K. C. Patil, J. Alloys Compd. **217**, 104 (1995).
[20] K. Uematsu, K. Toda, M. Sato, J. Alloys Compd. **389**, 209 (2005).
[21] G. Blasse, B. C. Grabmaier, Luminescent Materials. Springer, Berlin, 1994.

---

[*] Corresponding author: yangpiaoping@hrbeu.edu.cn